The effect of process parameters on grinding forces and acoustic emission in machining tool steel 1.2201/NC10
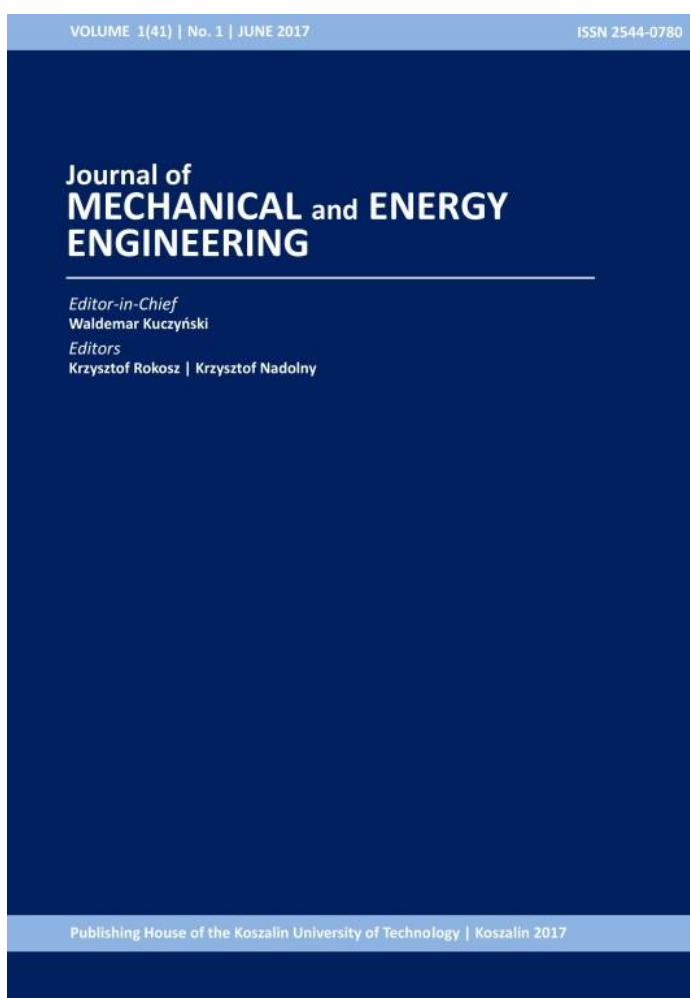
Paweł SUTOWSKI

THE EFFECT OF PROCESS PARAMETERS ON GRINDING FORCES AND ACOUSTIC EMISSION IN MACHINING TOOL STEEL 1.2201/NC10

Paweł SUTOWSKI

Koszalin University of Technology, Mechanical Engineering Department, pawel.sutowski@tu.koszalin.pl

Abstract: The article presents the association of the output signals of the grinding process with the machining parameters. The article focuses on assessing the suitability of grinding force signal and acoustic signal acquisition for different process conditions. In the first part of the article the kinematic contact of abrasive grain with the workpiece analysis was carried out. By analogy to the micro-cutting process, geometric analyses are presented and the process parameters that have a major impact on the grinding zone load are indicated. Analytically it has been shown that elementary grinding speeds (wheel and workpiece speed) and grinding depth have a significant effect on recorded signal values. The work also presents a set of factors and phenomena that are sources of acoustic emission impulses in the grinding process. For a selected range of grinding parameters, an experimental verification was performed. The article presents the highly correlated relationship between grain penetration depth (maximum uncut chip thickness) and grinding force components, as well as the effective value of acoustic emission. The output signals of the grinding process were also compared, indicating the advantage of the acoustic emission signal above the grinding force in terms of the reaction speed (and lag) of the sensors to the phenomena occurring in the grinding zone.

Keywords: grinding process, acoustic emission, grinding force, effective value

1. INTRODUCTION

Raising the quality of workpieces is one of the most important objectives in modern production systems, which supervise technological processes in real-time (on-line) is a must to ensure their continuous operation with high efficiency and quality. Generally, the grinding processes are diagnosed through multi-parametric measurements: the force components (normal and tangent), grinding power, vibration, surface temperature, acoustic emission, etc.

In the technological process, in most cases, grinding is a final machining operation, and which is additionally characterized by a significant randomness of its course and is subjected to wear of the abrasive tool. Therefore, precision and reliability of grinding process control is of particular importance. Therefore, more and more frequently, the use of relatively easy and not-destructive measurement techniques such as

acoustic emission measurement methods has been increasingly used to diagnose grinding processes.

Acoustic emission technique (AET) is a modern tool to monitor and diagnostic machining processes. It can be used to monitor events occurring during various processes, including grinding process. In case of non-contact sensors, like *Schall-Emissions-Hydrophon* (SEH) [1], rotating sensor (RSA, German *Rotierender Schallemissionsaufnehmer*) or inductive sensor (BSA, German *Berührungsloser Schall-emissionsaufnehmer*) acoustic emission technique can be applied even in difficult to monitor rotating processes, e.g. the cylindrical grinding [2].

Acoustic emission signal transcribe grinding wheel wear information [3]. AE can be used to evaluate selected surface geometrical structure parameters and for evaluation of stresses cumulated in the surface layer of the workpiece [4]. Couey et al. presented experimental results that indicate that force measurements are preferable to acoustic emission in precision grinding, since the force sensor offers

improved contact sensitivity, higher resolution, and is capable of detecting events occurring within a single revolution of the grinding wheel [5].

Some results show that there are obvious mapping relations between the technique parameters of grinding and the effective values of the AE signals. Han and Wu studied that after change of the parameters of grinding, the AE signals have the similar variation tendency as the forces in the process of grinding [6].

Therefore, in this paper an attempt was made to assess the suitability of the acoustic emission signal and the grinding force in the assessment of the surface grinding process.

2. KINEMATIC OF ABRASIVE CONTACTS AND SIGNAL SOURCES

Shaping the surface of a ground object is a kinematically conditioned removal of the material layer using the cutting ability of the active particles (cutting edges) of the grinding wheel active surface.

Abrasive machining is a stochastic process, in which cutting edges density (i.e., spacing between grains), the shape of cutting edges and the depth of the grains below the surface vary randomly.

Randomness is a source of variability in the behaviour of individual grains and in the micro-scale surface material removal process. In this case, the micro-cutting analogy is a good attempt to characterize average process behaviour [7].

When we assume the spacing between edges is equal to L, we can prove from geometric relationship, that the feed of workpiece per cutting edge is s:

$$s = L \cdot v_w / v_s. \tag{1}$$

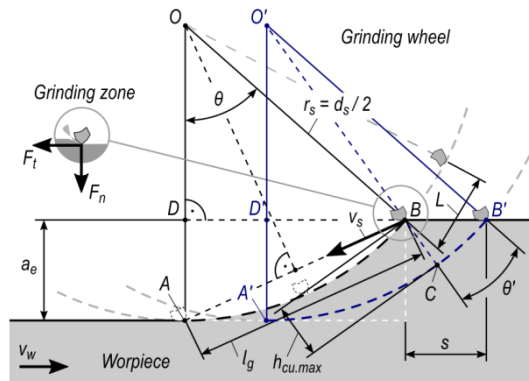These quantities and more, are illustrated in Fig. 1.

Fig. 1.   The geometry of micro-scale surface material removal process by single grains

The maximum thickness of the uncut chip ($h_{cu.max}$) and geometric contact length (l_g) can be enumerated as follows:

$$\sin \frac{\theta}{2} = \frac{\overline{AB}}{2} \cdot r_s^{-1} = \frac{\overline{AB}}{2 \cdot r_s}, \tag{2}$$

$$l_g = \overline{AB} = 2 \cdot r_s \cdot \sin \frac{\theta}{2}. \tag{3}$$

For small angles, where:

$$\sin \theta = tg\theta = \theta, \tag{4}$$

the equitation (3) is:

$$l_g = 2 \cdot r_s \cdot \frac{\theta}{2} = r_s \cdot \theta = \frac{d_s}{2} \cdot \theta. \tag{5}$$

And more:

$$\overline{BD}^2 + \left(\frac{d_s}{2} - a_e\right)^2 = \left(\frac{d_s}{2}\right)^2, \tag{6}$$

$$\overline{BD}^2 = \left(\frac{d_s}{2}\right)^2 - \left(\frac{d_s}{2} - a_e\right)^2, \tag{7}$$

$$\overline{BD}^2 = d_s \cdot a_e - a_e^2 = (d_s - a_e) \cdot a_e. \tag{8}$$

And finally:

$$\overline{AB}^2 = d_s \cdot a_e - a_e^2 + a_e^2 = d_s \cdot a_e, \tag{9}$$

$$l_g = \overline{AB} = \sqrt{d_s \cdot a_e}. \tag{10}$$

The grain penetration depth (maximum uncut chip thickness) we can make calculations as BC segment (from the triangle BCB' and D'O'B) that:

$$h_{cu.max} = s \cdot \sin(\theta - \theta'), \tag{11}$$

$$\sin(\theta - \theta') = \frac{D'B}{O'B} = \frac{\sqrt{a_e \cdot d_s - a_e^2} - s}{ds/2 - h_{cu.max}}, \tag{12}$$

$$h_{cu.max} = 2 \cdot s \sqrt{\frac{a_e}{d_s} - \frac{a_e^2}{d_s^2} - \frac{2 \cdot s^2}{d_s}}. \tag{13}$$

This equitation is usually simplified, since $(a_e)^2$ is much smaller than $(a_e \cdot d_s)$ and (s^2/d_s) is relatively small:

$$h_{cu.max} = 2 \cdot s \sqrt{\frac{a_e}{d_s}}. \tag{14}$$

The maximum thickness of the uncut chip is given by Eqns (1) and (14) with error less than 10%, which is acceptable for most purposes [7]:

$$h_{cu.max} = 2 \cdot \frac{L \cdot v_w}{v_s} \sqrt{\frac{a_e}{d_s}}. \tag{15}$$

The maximum thickness of the uncut chip is, therefore, a good determinant of main process parameters. The changes of grinding wheel diameter

(d_s) respond to radial wheel wear, the working engagement (a_e) is equivalent of tool load and determines observed values of normal force component (F_n) during process. The mean spacing between edges (L) is connected directly with wear mechanism of the abrasive grains (i.e., flattening, microcrystalline grain splintering, partial grain break-off, and total grain break-off) and it can be measured by mean width of the profile elements (*RSm*) value from surface profile of wheel.

Grinding forces are a key parameter in the grinding process, and workpiece speed, as well as wheel speed, takes main part in kinematics of grinding process. Both speeds determine grinding force and power. Due to the high speed of the wheel, the tangential force in grinding is mainly responsible for power and energy [7]:

$$P_s = F_t \cdot (v_s \pm v_w), \qquad (16)$$

$$E_s = \int_0^t F_t \cdot (v_s \pm v_w) \mathrm{d}t \cdot \qquad (16)$$

Directly influence on a_e parameter has normal force component (F_n), and its acts directly to reduce the depth of cut during machining. Most popular model of grinding force is Werner's model [8]:

$$F_n = K \cdot (C)^\gamma \cdot \left(\frac{v_w}{v_s} \right)^{2\varepsilon - 1} (a_e)^\varepsilon \cdot (d_s)^{1-\varepsilon} \cdot \qquad (17)$$

The normal force is also responsible for deflections of the workpiece of the abrasive tool (in the machine-workpiece-tool system), as well as depends on the bluntness of the abrasive grains on the surface of the abrasive tool [7].

Detailed analysis and modelling of cutting forces in grinding process considering variable stages of grain-workpiece micro interactions was presented by Li et al. [9]. The proposed method can be used to model grinding forces in detail, but also promising to study other grinding issues (e.g. grinding heat, machined surface topography, grinding chatter).

The acoustic emissions generated in the material by external influences are the process of producing an acoustic sound wave signal, propagated over the entire volume of material. Acoustic emissions are associated with a wide variety of phenomena, ranging from sub-microscopic phenomena such as the diffusion of atoms to an adjacent position in the crystal lattice and ending with macroscopic scale processes (e.g. catastrophic destruction) [10].

The main source of the AE signal in the grinding process is the grinding zone. Each abrasive grain in contact with the ground is subjected to an explosion of the AE impulse, which propagates through the grinding wheel and material.

An individual abrasive grain passes through the contact zone (l_g) at grinding wheel speed (v_s) and the time of contact. The tribological implications of grinding process shows that there are three different times of contact between an abrasive grain and workpiece surface [7]. First is when the abrasive tool enters contact with the workpiece and remains in contact until the workpiece has moved a distance equal to the contact length l_g (the contact time is l_g/v_w and typically has a magnitude 10 ms). Second is when an individual abrasive grain passes through the contact zone at wheel speed v_s (the time of contact as the grain passes through is l_g/v_s). For typical values: $l_g = 0.5$ mm and $v_s = 30$ m/s, it is 16 µs. So, each active grain, makes impact with surface with about 60 kHz frequency. During the sum of these short grain interactions, the total energy of the process takes place. The last case is when grain passes a point on the workpiece at wheel speed but only remains in contact for an extremely short distance and time (no larger than 15 µm and 0.5 µs). This correspond to 2 MHz events.

Main sources of acoustic emission impulses in grinding zone are presented in Fig. 2.
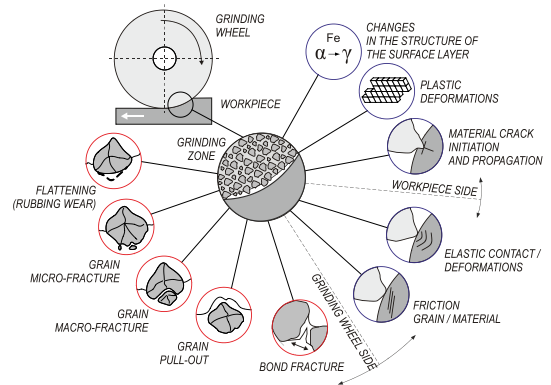

Fig. 2.   Main sources of acoustic emission impulses in grinding zone

The most significant are abrasive grain and bond wear phenomena, which are responsible for most energy AE impulses generation. Symptoms of wear of the abrasive grains and the bond are primarily abrasion and cracking. Bond bridges are mainly prone to cracking, while the abrasive grains are subject to a more complex process of wear. In this case, we distinguish between the following forms of wear: flattening and rubbing wear, micro-fracture, fracture of larger particles (macro-fracture), removal of grains from the bond (associated with fracture of the bond bridges).

Other sources of acoustic emission impulses are three stages of material deformation as a grain interacts with a workpiece: rubbing, ploughing and cutting. Rasim et al. described the chip formation in grinding process in detail in [11]. The phases of chip formation in grinding are presented in Fig. 3.
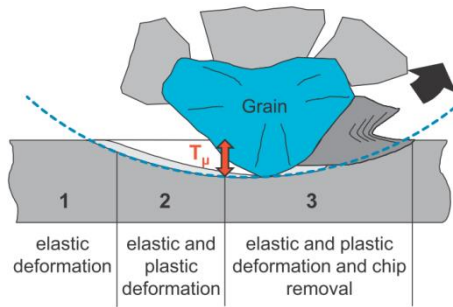
Fig. 3.   Phases of chip formation in grinding [11]

During rubbing the material is mainly deformed elastically — first contact between grain and material friction caused elastic material deformation. Ploughing and cutting takes place when the grain penetrates deeper into the workpiece. By increasing the penetration depth (specific grain cutting depth T_μ), the material removal is enhanced due to increased forces and a chip is formed.

It is obvious that, depending on the wear intensity of the grinding wheel, the proportion of phenomena associated with plastic deformation, friction and cracking will be different. It may happen that, despite the differences in grinding wheel wear, grinding forces will have comparable values. On the other hand, acoustic emission signals will more clearly illustrate the nature of work and wear of the abrasive grains.

3. MATERIALS AND METHODS

The study objects were samples (100×20×8 mm) made of tool steel 1.2201 (EN — X165CrV12, PN — NC10). This is cold working steel and it is used for industrial punches, knives and stickles, as well as on dies for the plastic cold deformation. It contains a lot of carbon and chromium and austenite after hardening from the high temperature.

Table 1 presents the chemical composition and mechanical properties of this material. More information about this material and influence of nitrogen ion implantation on tribological properties can be found in [12].

Tab. 1.   Chemical composition and mechanical properties of the 1.2201/NC10

C (wt.%)	Si (wt.%)	Mn (wt.%)	P (wt.%)
1.55–1.75	0.25-0.40	0.20-0.40	max. 0.035
S (wt.%)	Cr (wt.%)	V (wt.%)	Yield $R_{p0.2}$ (MPa)
max. 0.035	11.0-12.00	0.07-0.12	295 ($\geq$)
Tensile R_m (MPa)	Impact KV/KU (J)	Brinell hardness (HBW)	Elongation A (%)
641 ($\geq$)	23	141	34

Experimental experiments were carried out on a flat grinding machine OC3 model 3771 (Union of Soviet Socialist Republics) with an alumina grinding wheel 1-250×32×98-99A60J7V (INTER-DIAMENT, Poland). The grinding wheel was dressed prior to each series of tests, with a single grit diamond dresser in several transitions with transverse stroke of 280 mm/min and dressing depth of 0.30 mm. Variable machining parameters were used in the study: wheel speed v_s = 35, 32.5, 30, 27.5 and 25 m/s, longitudinal feed rate of workpiece v_w = 4, 9, 14, 19 and 24 m/min and grinding depth a_e = 0.01, 0.02, 0.03 and 0.04 mm. By creating a research plan, it was decided to select the machining parameters based on the experiment plan, which was a randomized Youden's Rectangle (SPRYR) — Table 2.

Tab. 2.   Grouped grinding process parameters

Common parameters			
f_a = 0.3 mm/rev, Q_f = 3 l/min (0.05 l/s)			
Series	a_e, mm	v_s, m/s	v_w, m/min
1	0.01	30	4
		27.5	9
		25	14
		35	19
		32.5	24
2	0.02	27.5	4
		25	9
		35	14
		32.5	19
		30	24
3	0.03	25	4
		35	9
		32.5	14
		30	19
		27.5	24
4	0.04	35	4
		32.5	9
		30	14
		27.5	19
		25	24

The components of the grinding force and the high frequency acoustic signal were measured in the studies.

The measurements of the normal F_n and tangential F_t components of grinding force were made with the use of a 3-component dynamometer type 9251A and 5019A amplifier (Kistler Holding AG, Switzerland). The AE signals were measured by low noise acoustic emission sensor (SEA, German Schaeff-Emissions-Aufnehmer). Piezotron® 8152B (produced by Kistler Holding AG, Switzerland) worked in the 0.05 to 1.0 MHz frequency range. Converter 5125B2 (Kistler Holding AG, Switzerland) with high-pass filter (HPF) 50 kHz and low-pass filter (LPF) 1000 kHz was used

in the measurement system as well. Filtering process made it possible to cut-out most of the vibrations and machine noises from AE signals. The converter was used also to calculate the effective value of the signal $AE_{eff.}$ (with integration constant $\tau_{rms} = 0.12$ ms).

The signals were acquired using PXIe-6124 16 bit converter with a sampling frequency 2.5 MHz per channel.

During the experimental tests, workpiece was mounted to dynamometer by special holder, and acoustic sensor was attached directly to the workpiece.

4. RESULTS AND DISCUSSION

Under the accepted test conditions, the grinding process proceeded with considerable variation in average cutting depth per abrasive grain (Fig. 4). This was the result of the grinding parameters, mostly: a_e, v_w and v_s.
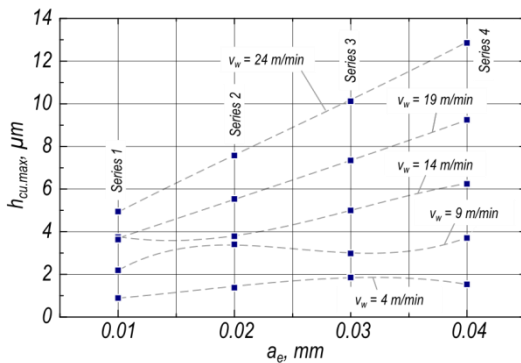

Fig. 4. The variability of the maximum thickness of the uncut chip ($h_{cu.max}$) for process parameters set out by SPRYR statistic

To set values of the maximum thickness of uncut chip, the mean distances between grain vertices, measured from the profile of the active surface of the grinding wheel, were taken into consideration. The variability of the spacing between edges (for active grains) is presented in Fig. 5.
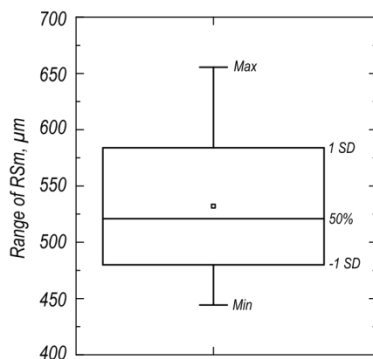

Fig. 5. The variability of the spacing between edges (active grains) assumed as mean width of profile elements

The changes in elemental depth of cut significantly affect the character of the deformation in the micro-cutting zone, which is reflected by the immediate response of the F_n and F_t signals, as well as the AE signal that is presented in Figs. 6–8.
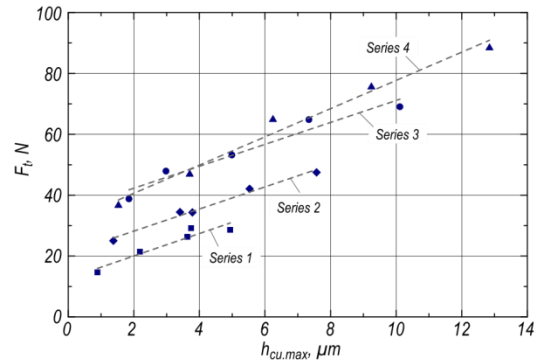

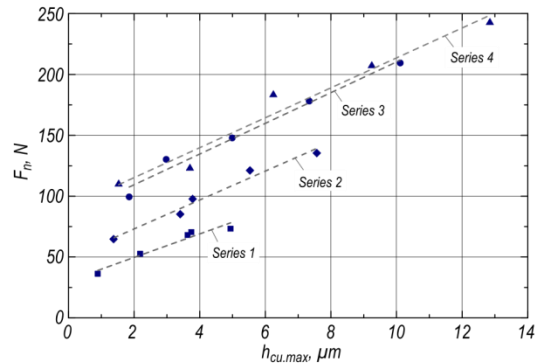Fig. 6. Variability of the tangent component of the grinding force according to the machining conditions

Fig. 7. Variability of the normal component of the grinding force according to the machining conditions

From the analysis of both graphs, it is clear that the measurements of the components of the grinding force are sensitive in this regard. As the grain load increases, both the normal and tangential components grow. The normal component of the grinding force varied between 50 N and 150 N, while the tangential component increased proportionally from 20 N to 100 N. This gives grinding force ratio equal to $\mu = 0.4$, what is typical value. In both cases, the increase in grinding force depends on the v_w and v_s speeds, and the rate of this increase is constant (slope of the curves).

The basic linear regression model has been used to fitting curve ($y = a + b \cdot x$) in the case of grinding force components. The quality of linear regression has been measured by the adjusted coefficient of determination, reduced Chi-square value, which equals the residual sum of square divided by the degree of freedom, and then using the F-test.

Fitting results between tangential component of grinding force and maximum thickness of the uncut chip are presented in Table 3.

Tab. 3. Fitting results between tangential component of grinding force and maximum thickness of the uncut chip

Series	*a* value	*b* value	Reduced Chi-Sqr	Adj. R-Square	F value
1	12.6	3.69	4.82	0.87	312
2	20.9	3.63	1.45	0.98	2411
3	35.1	3.60	10.1	0.93	770
4	31.3	4.64	11.6	0.97	911

The fit of the all regression functions is very good (Adj. R-Square in the range of 0.87 to 0.98), which means that those models are appropriate for the data. The reduced chi-squared value and the F value additionally indicate that the model parameters are statistically significant. This means that the estimated models can be used to determine the value of the grinding force based on $h_{cu.max}$, i.e. grinding parameters and grinding wheel geometry.

Similar results were obtained for normal component of grinding force — Table 4.

Tab. 4. Fitting results between normal component of grinding force and maximum thickness of the uncut chip

Series	*a* value	*b* value	Reduced Chi-Sqr	Adj. R-Square	F value
1	30.3	9.66	18.4	0.92	516
2	49.3	11.9	28.3	0.96	951
3	90.6	12.3	157	0.95	516
4	84.1	12.6	48.0	0.97	1291

For different grinding depths (a_e), at constant $h_{cu.max}$ values, the AE signal takes values in the larger scattering bands (Fig. 8). This is due to the fact that the effective value of the acoustic signal not only takes into account the variation of the elementary cutting depth but also provides information on the interactions of the tips of the grains that did not initiate the cutting process but are already in contact with the material surface.

Additional sources of acoustic emissions include vibrations, i.e. vibrations from machine (rolling bearing, fast motions, hydraulics), and other sources from environment, e.g. impulses created by cooling lubricant or operator behaviour.
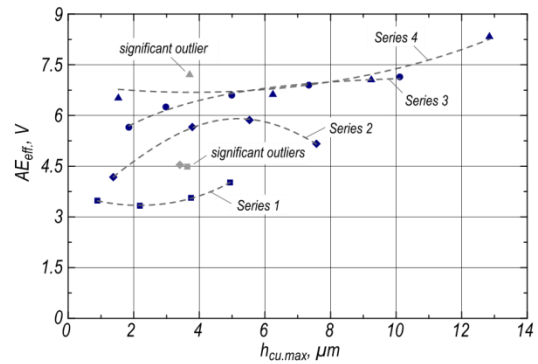

Fig. 8. Mean value of the AE signal according to the machining conditions

Exponential functions have been chosen as fitting models for $AE_{eff.}$ signal. For research series number 1, 2 and 4 it was three-coefficients function ($y = \exp(a + b \cdot x + c \cdot x^2)$), and for series number 3 — an asymptotic regression model ($y = a - b \cdot c^x$).

In all cases, the fit succeeded. Chi-square was reduced and the tolerance was reached. This means that the maximum likelihood estimates of the parameters have been obtained (by minimizing the chi-square value). Fitting results between effective value of AE and maximum thickness of the uncut chip are presented in Table 5.

Tab. 5. Fitting results between effective value of AE and maximum thickness of the uncut chip

	Series 1	Series 2	Series 3	Series 4
a value	1.32	1.14	7.19	1.94
b value	-0.10	0.25	2.74	-0.02
c value	0.02	-0.02	0.72	0.003
Reduced Chi-Sqr	5E-4	0.001	0.009	0.19
Adj. R-Square	0.99	0.99	0.97251	0.62
F value	34654	32746	7586	433

The regression models show that the effective value of the acoustic emission signal is affected much more factors than is the case with grinding force components.

Individual events such as cracking of the abrasive grains have a significant effect on the measurements obtained from the grinding zone. On the other hand, the distribution of data for the components of the grinding force is more damped — their course is within the smaller range of variation for all series of tests. In addition, with respect to the AE signal, it can be observed that the force signals are recorded with clear delay (Fig. 9).
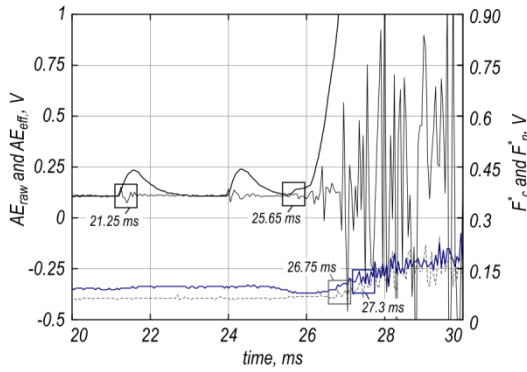
Fig. 9. Comparison of delay response of measuring system during recording the first contact of grain with workpiece and the beginning of grinding process

The AE signal gives a much faster response (with shorter delay time) to changes in the grinding zone than detection system based on grinding force sensors. The results of analysis of the signal lags are presented in Table 6.

Tab. 6. Grouped grinding process parameters

Quantity	Event detection time point	Lag (to FC / GP)
Acoustic emission (AE_{raw} and $AE_{eff.}$):		
— First contact (FC)	21.25 ms	—
— Grinding process (GP)	21.65 ms	—
Normal component of grinding force (F_n)	26.75 ms	5.50 / 1.10
Tangential component of grinding force (F_t)	27.30 ms	6.05 / 1.65

In the initial processing phase, AE sources can be clearly identified, and consequently, the raw signal (AE_{raw}) and the energy produced in the form of the measured value ($AE_{eff.}$) are altered in very clear and rapid way. At that time, the values of the grinding force components showed no change or increased with considerable delay compared to the AE signal. The lack of response of the grinding force sensor to the incident indicates the superiority of the AE signal monitoring system over the systems without such sensors. In this case, the lag of the grinding force sensor response is significant and is approx. 5–6 ms.

Also, when the abrasive grains are approaching the grinding zone, the level of the acoustic emission signal is clearly increasing. This is triggered by a shock wave that is generated by the turbulent flow of air and coolant in the gap between the surface of the grinding wheel and the workpiece.

5. CONCLUSIONS

The analysis and the results of the experimental studies indicate the possibility of using the AE signal and the components of the grinding force to effective monitor grinding process.

Signal values are dependent on the grinding depth (working engagement) and other processing parameters.

The set out dependencies between the signals recorded during grinding and the loading of the grinding zone (as a result of the application of different parameters and variable maximum thickness of the uncut chip) allow the development of a grinding monitoring system that allows adaptive control of the grinding process. Due to the need to include the abrasive tool wear in such a system, a neural network process model should be developed that would recognize non typical cases of process instances.

Inclusion in monitoring system both the AE and grinding force signals is expected, because of the unique link those signals with process parameters, particularly in the case of grinding force components.

Nomenclature

Below were given most important symbols and acronyms used in article.

Symbols

a_e – depth of cut (working engagement), mm
C_1 – the cutting edge density, $1/mm^2$
d_s – grinding wheel diameter, mm
f_a – axial feed speed, mm/rev
F_n – normal component of grinding force, N
F_t – tangential component of grinding force, N
$h_{cu.max}$ – maximum thickness of the uncut chip, μm
K – proportionality factor,
L – mean grain spacing along motion, μm
l_g – geometric contact length, mm
P_s – processing power, W
Q_f – coolant flow rate, l/min
r_s – grinding wheel radius, mm
RSm – mean width of profile elements, within a sampling length, μm
s – feed of the workpiece per cutting edge, μm
T_μ – specific grain cutting depth, μm
v_s – grinding wheel peripheral speed, m/s
v_w – axial table feed speed (workpiece speed), m/min

Greek letters

γ – exponent taking values form 0.5 to 1,
ε – exponent taking values form 0.5 to 1,
θ – angle subtended by the arc of contact on the wheel, rad
θ' – angle subtended by an angular rotation, rad
μ – grinding force ratio

Acronyms

AE – Acoustic Emission
AET – Acoustic Emission Technique
BSA – Berührungsloser Schallemissionsaufnehmer
RSA – Rotierender Schallemissionsaufnehmer
SEH – Schall-Emissions-Hydrophon
SPRYR – Static Program Randomized Youden's Rectangle

References

1. Sutowski P., Nadolny K., Kapłonek W. (2012). Monitoring of cylindrical grinding processes by use of a non-contact AE system. *International Journal of Precision Engineering and Manufacturing*, Vol. 13, No. 10, pp. 1737-1743. http://dx.doi.org/10.1007/s12541-012-0228-7.
2. Sutowski P., Plichta S. (2006). Zastosowania metody pomiaru emisji akustycznej w ocenie procesów obróbkowych [Application of acoustic emision measurement method to evaluation of machining process]. *Przegląd Mechaniczny*, Vol. 2, pp. 20-25.
3. Sutowski P. (2010). Oszacowanie stopnia zużycia ściernicy z wykorzystaniem sygnału emisji akustycznej i teorii zbiorów rozmytych [The evaluation of grinding wheel wear with use of acoustic emission signal and fuzzy logic system]. *Archiwum Technologii Maszyn i Automatyzacji*, Vol. 30, No. 4, pp. 47-56.
4. Sutowski P. (2012). Surface evaluation during the grinding process using acoustic emission signal. *Journal of Machine Engineering*, Vol. 12, No. 4, pp. 23-34.
5. Couey J.A., Marsh E.R., Knapp B.R., Vallance R.R. (2005). A Comparison of Force and Acoustic Emission Sensors in Monitoring Precision Cylindrical Grinding. In: SPIE Proceedings Vol. TD03, Optifab, Technical Digest, 2 May 2005. DOI: 10.1117/12.605545.
6. Han X., Wu T. (2013). Analysis of acoustic emission in precision and high-efficiency grinding technology. *The International Journal of Advanced Manufacturing Technology*, Vol. 67, No. 9, pp. 1997-2006. doi:10.1007/s00170-012-4626-x.
7. Ioan D., Marinescu W., Rowe B., Dimitrov B., Ohmori H. (2013). *Tribology of Abrasive Machining Processes* (Second Edition), William Andrew Publishing, Oxford, ISBN 9781437734676, https://doi.org/10.1016/B978-1-4377-3467-6.00001-X.
8. Werner G. (1978). Influence of work material on grinding forces. *Annals of* CIRP, Vol. 27, No. 1, pp. 243-248.
9. Li H.N., Yu T.B., Wang Z.X., Zhu L.D., Wang W.S. (2017). Detailed modeling of cutting forces in grinding process considering variable stages of grain-workpiece micro interactions. *International Journal of Mechanical Sciences*, Vol. 126, pp. 319-339. https://doi.org/10.1016 / j.ijmecsci.2016.11.016.
10. Grosse C. U., Ohtsu M. (2008). *Acoustic emission testing: Basics for Research-Applications in Civil Engineering.* Springer Berlin Heidelberg. DOI: 10.1007/978-3-540-69972-9.
11. Rasim M., Mattfeld P., Klocke F. (2015). Analysis of the grain shape influence on the chip formation in grinding. *Journal of Materials Processing Technology*, Vol. 226, pp. 60-68, https://doi.org/10.1016/j.jmat protec.2015.06.041.
12. Budzyński P., Tarkowski P., Penkała P. (2001). Influence of nitrogen ion implantation on tribological properties of tool steel NC10. *Vacuum*, Vol. 63, No. 4, pp. 731-736. https://doi.org/10.1016/S0042-207X(01)00266-4.

Biographical note

Paweł Sutowski received his MSc degree in Mechanics and Machine Design and PhD (with honors) degree in Machinery Construction and Operation from Koszalin University of Technology, in 2001 and 2008, respectively. Since 2008 he has didactic-research position in the Department of Production Engineering at the Koszalin University of Technology, where currently he works as an Assistant Professor in production planning and control team. His scientific work focus on problems concerning quality and efficiency control of machining processes by monitoring and diagnostic output signals. In his work, he uses modern signal acquire and converting unit systems. The most important in his work are non-destructive testing (NDT) methods with the use of acoustic signal and others. He has participated in national research projects, presenting results of his work at international and national conferences. He has published scientific papers in international and national journals, book chapters, as well as conference proceedings. He is also the co-author of one monograph. In his professional work he was also experience in domestic and foreign industry. He was a CAD designer (Satrorius AG in Germany, GIPO Corp. in Denmark and Poland), as well as software programmer and commercialize (ZETO S.A. in Poland).